A national laboratory of the U.S. Department of Energy
Office of Energy Efficiency & Renewable Energy

National Renewable Energy Laboratory

*Innovation for Our Energy Future*

# Tolerance of Three-Stage CIGS Deposition to Variations Imposed by Roll-to-Roll Processing

## Final Technical Report
## May 2003 – September 2005

M.E. Beck and J.S. Britt
*Global Solar Energy, Inc.*
*Tucson, Arizona*

***Subcontract Report***
**NREL/SR-520-39119**
**January 2006**

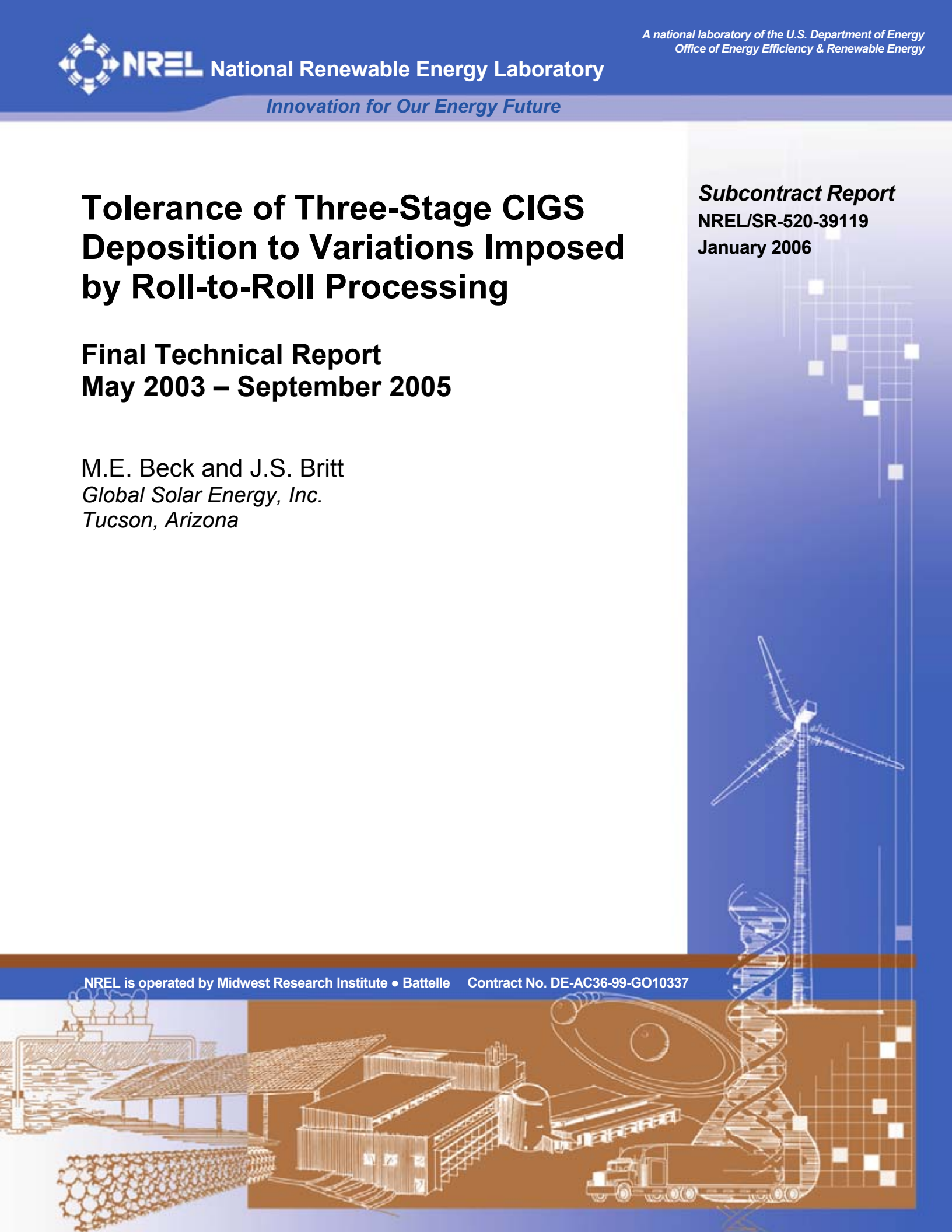

NREL is operated by Midwest Research Institute • Battelle Contract No. DE-AC36-99-GO10337

# Tolerance of Three-Stage CIGS Deposition to Variations Imposed by Roll-to-Roll Processing

*Subcontract Report*
**NREL/SR-520-39119**
**January 2006**

## Final Technical Report
## May 2003 – September 2005

M.E. Beck and J.S. Britt
*Global Solar Energy, Inc.*
*Tucson, Arizona*

NREL Technical Monitor: H. S. Ullal
Prepared under Subcontract No. ZDJ-2-30630-14

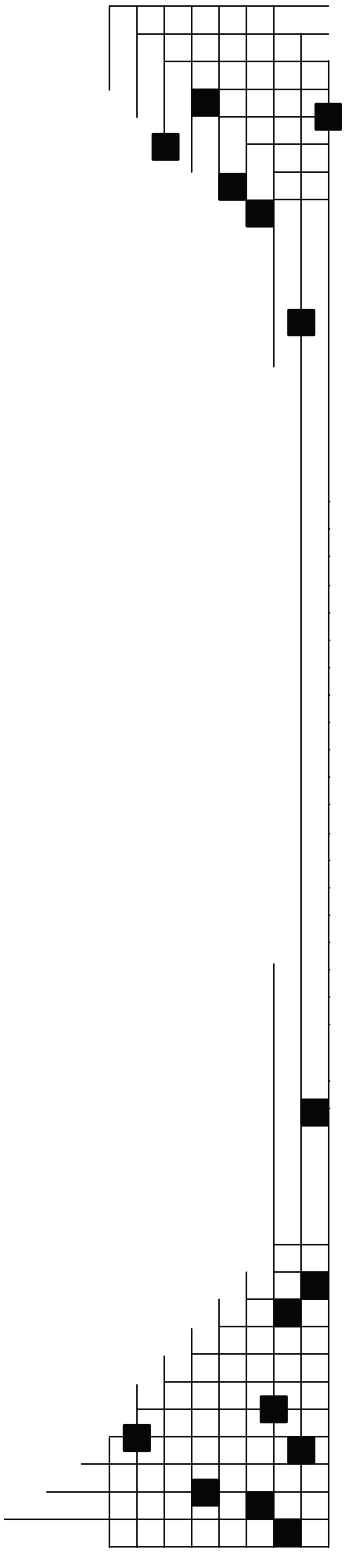

**National Renewable Energy Laboratory**
**1617 Cole Boulevard, Golden, Colorado 80401-3393**
**303-275-3000 • www.nrel.gov**

Operated for the U.S. Department of Energy
Office of Energy Efficiency and Renewable Energy
by Midwest Research Institute • Battelle

Contract No. DE-AC36-99-GO10337

# TABLE OF CONTENTS

## LIST OF FIGURES



## LIST OF TABLES

## Executive Summary

Two and three stage co-evaporation have come to be viewed as benchmark laboratory methods for $CuIn_xGa_{1-x}Se_2$ (CIGS) absorber deposition, having produced CIGS device efficiencies greater than 15% reproducibly in a number of laboratories. Although quite successful and relatively easy to implement on a small R&D scale, scale-up to a commercial level proves to be challenging. Yet, large area, continuous manufacturing processes represent the most economically attractive path for thin film PV commercialization. Large area, continuous processes necessarily differ substantially from laboratory methods, and direct use of the processes developed in the laboratory is not feasible. Differences are imposed both by continuous processing of moving substrates, and by requirements for decreased costs and increased throughput. For implementation of viable, large scale PV manufacturing methods on low-cost substrates it is necessary to understand the tolerance of the established laboratory processes to variations in deposition procedures, as they apply to low-cost roll-to-roll (RTR) processing onto lightweight stainless steel foils.

As a Technology Partner to NREL under the Thin-Film Photovoltaics Partnerships Program (TFPPP) the purpose of this subcontract was to move CIGS photovoltaics toward large-scale, cost-effective, manufacturing by examining the tolerance of three-stage deposition to changes in processing variables consistent with continuous RTR manufacturing at Global Solar Energy (GSE). The final objective of this work was the demonstration of commercial, low-cost and robust modules. Increasing production cell efficiency, as well as yield, represented the key aspects of this effort.

Prior to this three-year program, GSE had demonstrated average large area production device efficiencies in the 7-8% range with best devices greater than 10%. Goals under this TFPPP subcontract were to raise both numbers by 2 percentage points. Pre-contract production yield was 20% and was to be increased to 80%. All work proceeded as planed: production yield was improved to 90% while the average production efficiency has been raised to 10%, with peak efficiencies exceeding 13%.

During Phase I, a three-stage bell jar process was established at ITN, characterization of the GSE RTR production processes began, and the bell jar system was used to explore some sensitivities of the three-stage process. In Phase II, characterization of the GSE RTR production processes in terms of major variables was completed, further process sensitivities were explored in the bell jar, and application of process tolerance information to the roll-coaters began. Under Phase III efforts begun in Phase II were completed, verification at the production level conducted, production RTR processes refined, and impacts of feedstock purity on resulting device quality assessed.

More precisely, process sensitivities to the degree of Cu-rich excursion ($2^{nd}$ stage), final Cu/(In+Ga) ratio as well as Ga/(In+Ga) distribution were studied at the production level. Based on these experiments it was concluded that a maximum Cu ratio of 1.1 allows for a more robust process than a maximum Cu ratio of 1.0, while the latter may yield slightly higher absolute device efficiencies. As for the group III elemental distribution, various Ga/(In+Ga) profiles throughout the absorber yield maximum efficiencies, but a robust process can be achieved for a narrow profile only.

Furthermore, the parameter space of the Na-precursor deposition and Se delivery have been analyzed. The former was found to have a significant impact on absorber adhesion, while insufficient or excessive Se delivery resulted in device performance degradation. Back contact optimization efforts lead to reduced Cr diffusion into the absorber while simultaneously enhancing CIGS adhesion.

Finally, the cumulative efforts of this program lead to the conclusion that stationary bell jar experiments cannot adequately simulate the dynamics in roll-to-roll film growth. Further investigations of the process changes resulting from this work as to their impacts on product reliability, coupled with fine tuned, as well as cost-optimized production methods, form the cornerstones of future efforts at GSE.

# 1 Introduction

## *1.1 Background*

Two and three stage co-evaporation have come to be viewed as benchmark laboratory methods for $CuIn_xGa_{1-x}Se_2$ (CIGS) absorber deposition, having produced CIGS device efficiencies greater than 15% reproducibly in a number of laboratories. Although quite successful and relatively easy to implement on a small R&D scale, scale-up to a commercial level proves to be challenging. Yet, large area, continuous manufacturing processes represent the most economically attractive path for thin film PV commercialization. Large area, continuous processes necessarily differ substantially from laboratory methods, and direct use of the processes developed in the laboratory is not feasible. Differences are imposed both by continuous processing of moving substrates, and by requirements for decreased costs and increased throughput. For implementation of viable, large scale PV manufacturing methods on low-cost substrates it is necessary to understand the tolerance of the established laboratory processes to variations in deposition procedures, as they apply to low-cost roll-to-roll (RTR) processing onto lightweight stainless steel foils.

Only limited information is available in the literature addressing the tolerance of the laboratory processes to several variations. Some studies have been published related to CIGS thickness,[1] maximum deposition temperature and time spent by the film in the Cu-rich stage,[2,3] Na content,[4,5] rate profiles,[6] and final overall Cu/(In+Ga) atomic ratio.[7] Not only are there additional, at times more important, absorber characteristics that define the quality of the resulting absorber for use in a PV device, but these experiments were conducted without correlation to practical commercial fabrication methods. Further variations to the deposition procedure may be encountered in the manufacturing environment and include:

- Significantly shortened overall deposition times,
- Instantaneous variations in the Se/metals flux ratio outside the typically-recommended envelope due to spatial distribution of metallic flux,
- Impurities expected from less expensive, less pure source materials or alternative substrates,
- Deviation of substrate temperature from the prescribed two- and three-stage values,
- Variation in the fraction of group III elements deposited in the first versus third stages,
- Variations in sample cool-down procedures and post-CIGS handling, and
- Exposure to species outgassed and reflected from hot chamber walls.

During the course of this subcontract, Global Solar Energy, Inc. (GSE) and lower-tier subcontractor ITN Energy Systems, Inc. (ITN) addressed these process tolerance issues. The definition and resolution of process tolerance issues satisfy many of the goals of the Thin Film Photovoltaics Partnerships Program (TFPPP). First, the investigation identified acceptable ranges for critical deposition parameters, providing upper and lower control limits for in-situ process monitoring components, thus increasing average efficiency as well as yield of product. Second, the exploration uncovered insensitivities to some processing procedures, allowing module manufacturing at increased throughput and decreased cost. The exploration allowed for a quantitative evaluation of the trade-offs between performance, throughput, and costs. Third, the program also satisfied the TFPPP goal of establishing a wider research and development base for higher-efficiency processing. Fourth, the acquisition of data defining sensitivity to processing has important implications for the required accuracy of process sensors and control. Finally, the program aided the photovoltaic community advance toward a better understanding of CIGS growth, a longer-term goal of the TFPPP.

Three-stage co-evaporation of CIGS imposes stringent limits on the parameter space if high efficient devices are to result. Substrate temperatures during the 1st stage as well as during the 2nd and 3rd stage, Se partial pressure, and amount of Na supplied are critical for good nucleation, proper In-Ga-selenide precursor phase, and diffusion of Cu into the precursor as well as diffusion of Ga through the film. In addition, the degree of Cu-rich excursion impacts maximum performance and process tolerance. Enveloping the above is the basic time-temperature profile inextricably linked to the metals delivery rates. While high efficiency, three-stage deposited CIGS devices on the R&D scale are grown at about 20-45 minutes to thicknesses of 2 to 2.5 μm, the latter is not a viable approach for an economic manufacturing process. At GSE, CIGS films are typically grown in about

6 minutes to thicknesses of less than 2 μm. At the same time, the emissivity and thermal conductivity of SS is vastly different from that of glass, and the reduced growth time poses restrictions on the substrate temperature ramp rates and diffusion of species (reaction kinetics). Material compatibility in the highly corrosive Se environment places limitations on the substrate heaters; i.e., substrate temperatures. Finally, one key advantage of a RTR deposition approach (compact equipment) restricts post CIGS Se exposure and cool down rates to be vastly different than those practiced in the laboratory.

To form a complete picture of conditions in the production systems, metals flux profiles as a function of Se pressure were documented once the Se impingement rates were derived from in-situ sensor data. Time-temperature profiles for the substrate were measured using substrate equipped with temperature sensors processed through a production coater.

Utilizing the stationary deposition in the bell-jar, the following process variations on device performance were quantified: CIGS cool-down rate, cool-down Se flux, venting temperature, maximum Cu ratio during film growth and final Cu-ratio. Related to the production systems, the following topics were investigated: process robustness and device performance as a function of maximum and final Cu ratio and real-time sensing of maximum Cu ration.

In order to minimize losses due to reduced absorber thickness, GSE worked closely with the substrate vendor to improve the surface finish of the metal foil. Reductions in surface roughness minimized shunting and impurity outdiffusion via spikes not covered with the back contact layer. At the same time, different back contact layer thicknesses as well as alternate diffusion barrier materials were investigated as to their effectiveness against Fe outdiffusion.

As for the amount of Na present in the film. Stainless steel, as opposed to soda lime glass, does not provide intrinsic Na doping and Na needs to be added during film growth. GSE choose to accomplish this via in-situ evaporation of a thin Na precursor preceding the 1$^{st}$ stage of the absorber formation. However, the amount of Na added impacts CIGS to Mo adhesion. The interactions of Na, Mo and Se with In and Ga are complex and it is critical that the degree of Mo selenization is optimal for both good adhesion and ohmic contact. Using tape peel adhesion, different Na precursor thicknesses impacts on CIGS to Mo adhesion and device performance were investigated, while the more complex interactions of Na with Mo, In, Ga and Se as a function of substrate temperature are still under investigation.

Feedstock costs, most prominently those for In, are of concern with respect to reduced manufacturing costs. To a varying degree, the total feedstock cost for any given element (Cu, In, Ga, Se) is a function of the material as well as processing, including purification. The less pure, the more economical the feedstock becomes. However, solid-state CIGS-based devices are sensitive to certain impurities. Hence, if electrically active impurities are added via feedstock contamination, device efficiency would degrade offsetting the cost benefits associated with less pure feedstock. To this end, GSE procured the metals at three different purity levels and investigated the impact on device performance at the R&D level. It was found that GSE utilizes metal feedstock in the optimum range.

In addition to aspects of the CIGS deposition, challenges exist in the post-CIGS treatment steps. For example, while certain in-situ monitoring capabilities have been developed at GSE, a more detailed post-CIGS characterization is still desired and beneficial. However, this results in exposure of the CIGS to ambient for extended periods of time, leading to surface oxidation. Time resolved studies of ambient exposure as well as dry $N_2$ storage controls prior to CdS buffer deposition revealed the effect magnitude of ambient exposure on device performance. The penalty suffered from prolonged exposure was found to be minimal.

CdS absorbs photons that could otherwise be utilized for charged carrier generation within the absorber. Thinning the CdS layer to a level where blue light absorption is minimized was found to have far less of an impact than theoretically predicted. On the other hand, too thick a CdS layer was found to adversely impact short circuit current densities. The challenge, in particular on a rough substrate as opposed to the smooth surface of glass substrates, is that a thicker CdS buffer layer reduces shunting in the device. The latter aspect was circumvented via optimizing the CdS thickness in combination with the wider band gap intrinsic ZnO layer thickness.

Improved device performance has been reported to be attainable via surface sulfurization. GSE executed several experimental matrices, but was unable to reproduce the beneficial effects reported in the literature. Although

only minute amounts of Cd are contained in the device stack, significant reductions or even replacement may be possible via a partial electrolyte treatment using Cd or Zn. Exploring a wide parameter space, GSE was once again unable to achieve the benefits reported in the literature. Hence, efforts were focused on optimizing the chemistry and kinetics of the CdS process.

## *1.2 Technical Work Plan*

The research effort was structured to progress through three phases. The key elements of each phase were as follows:

**Phase One**

- **Establish Three-Stage Bell-Jar Process.** Establish the NREL-developed three-stage co-evaporation process in a bell jar at ITN; demonstrate satisfactory reproducibility and control on both glass and steel substrates.
- **Characterize Metals Flux.** Characterization of the shape of the metal profiles from the production evaporation sources. Assess the magnitude of effects of Se background pressure and deposition rate variations on the shape of the metal plume from the sources.
- **Temperature and Time Process Tolerance.** Utilizing the three-stage bell-jar process explore the effect of decreased processing time on CIGS film quality for multiple temperatures both on glass and steel substrates.

**Phase Two**

- **Selenium and Temperature Profiles.** Characterization of the shape of the Se distribution in the production evaporation sources. Characterize the flexible substrate temperature as a function of source temperature, heater temperatures, and web speed.
- **Process Tolerance for Deposition Species Fluxes and Temperatures.** Using the three-stage bell-jar process examine the effect of momentary variations in Se/metals fluxes, division of In and Ga between first and third stages, Cu-rich excursion of stage two, and processing temperature variations.
- **Identification of Critical Roll-to-Roll Conditions.** Identify areas where process improvements are possible, based on the sensitivities and characterization from previous tasks. Design deposition condition changes to increase yield and efficiency in the production roll-coaters.

**Phase Three**

- **Process Tolerance for Impurities and Device Finishing.** Via the three-stage bell-jar process examine the effect of chamber conditions during CIGS cool-down, the effect of impurities from source material and hot chamber surfaces, and the effect of handling procedures before CdS deposition.
- **Implementation of Process Improvements.** Implement process improvements in the production roll-coaters based on the results from the previous tasks. Verify the predicted dependencies via depositions in the roll-coaters.

All bell-jar related tasks were performed at ITN Energy Systems under supervision of Dr. Ingrid L. Repins. In order to optimize the amount of information in a given experiment under consideration of resources spend, GSE realizes the benefits inherent to the design of experiment approach in its studies. Prior to executing any given test, the list of variables and levels are considered and matched to the design deemed most appropriate. While typically several levels and variables are examined, it may be prudent to conduct screening experiments or even resort to one-variable at the time tests prior to launching a more complex design. Due to the number of inextricably linked variables more complex designs need to account for limitations such as response time (e.g., number of conditions obtainable on a 1000 ft. web) or equipment capabilities (e.g., maximum T setpoint) and it is not always possible to eliminate confounding effects. Replicas within the experiment as well as complete repetitions of an experiment further improve the quality of the statistical analysis.

### *1.3 Technical Approach*

In the approach pioneered by GSE, continuous rolls of stainless steel foil substrate as long as 1000-1200 feet are deposited with thin film PV layers, as opposed to individual small glass plates. Flexible, lightweight CIGS-based PV modules are fabricated by a novel interconnect method that avoids the use of wires or foils and soldered connections. Roll-to-roll vacuum deposition has significant advantages that translate directly into reduced capital costs, greater productivity, improved yield, greater reliability, lower maintenance, and a much larger throughput of PV material as compared to rigid plate processing.

However, historically very little effort has been directed toward the deposition of CIGS onto alternate substrates, such as metal foils. Only recently has there been some interest in understanding the aspects and challenges of the latter on a fundamental level and in comparing the parameter space to that of the traditional formation of CIGS on glass substrates. As such, GSE could not draw on previously and independently established fundamental studies in this area. Although not part of this contract, GSE developed manufacturing capabilities enabling the RTR process for CIGS on polymer and metal foils in a pioneering role. Under the prior TFPPP subcontract – *"Process Development of Large Area Thin Film CIGS"*, ZAK-8-17619-04, 2/98 - 12/01 – GSE was able to establish the parameter space for successful CIGS deposition on stainless steel foil. However, lack of sufficiently well resolved process control precluded work addressing process sensitivities to variations in the numerous process variables.

Concurrent with developing improved process control capabilities under the PVMaT subcontract – *"Photovoltaic Manufacturing Cost and Throughput Improvements for Thin-Film Based CIGS Modules"*, ZAX-8-17647-11, 7/98 - 11/01 –, the approach under this TFPPP subcontract centered around first establishing fundamental process sensitivities of CIGS depositions onto stationary substrates. This included metal and Se flux profile characterization and the interactions of the species in the plume. Process conditions encountered during the accelerated RTR deposition rates (web speed up to 12 in/min) in GSE's production scale equipment were mapped into the laboratory equipment. After establishing a bell-jar baseline process for deposition on glass, conditions were altered to reflect conditions representative of the stainless steel foil substrates in the RTR manufacturing equipment at GSE, including partial Se pressure, metal flux rates, time-temperature profiles, Cu-rich excursion, group III ratios, Na content etc. Process tolerances were explored and lessons learned were transferred to the production equipment. Final process optimization was then conducted at the manufacturing scale.

Besides the focus on the absorber formation process, process tolerances were also explored for the back contact sputter deposition, CdS buffer formation, and sputter deposition of the i-ZnO/ITO window layer.

## 2 Maximum Cu Ratio During CIGS Growth

### *2.1 Bell Jar Studies*

Bell-jar-scale experiments conducted during Phase II found the maximum Cu ratio during CIGS growth to have a large effect on device performance. Similar studies in the roll-coaters to reproduce these observations were ambiguous. Thus, the bell jar experiments were extended to include both, a more precise reproduction of the Ga profile in the production devices, and an experimental matrix allowing determination of statistical uncertainties. Maximum Cu ratio was again found to have a significant effect on device performance. The new data, analysis, and implications for production are described below.

Several studies have examined the impact of a Cu-rich growth period during three-stage CIGS co-evaporation.[2,3.7,8,9] Some of these studies have linked the Cu-rich growth period to larger grain growth and beneficial effects on device performance, while others have defined these benefits as limited to depositions at reduced temperatures or times. In general, conclusions in these studies are based on several pair-wise comparisons of depositions (e.g., comparisons of a sample with Cu-rich growth and another without for several deposition conditions) and have not included a statistical analysis of uncertainties. In this study, a designed[8] experiment utilizing 12 substrates and 144 devices was performed. For these films deposited on glass at 575°C over approximately 20 minutes, it was found that a Cu-rich growth period yields a statistically significant benefit for device performance through open-circuit voltage. By varying film thickness, the number of atoms deposited in stage 3 was also included as a variable in the experiment. The data indicated that device efficiency does not depend significantly on the number of moles deposited in stage 3.

CIGS films were deposited by three-stage co-evaporation onto 3" × 3" Mo/glass substrates in the ITN bell jar. A thermopile was used to monitor film emissivity and thereby deduce Cu-ratio (i.e., the atomic ratio Cu/[In+Ga]) in real time. Electron impact emission spectroscopy rate monitoring was used to control the number of moles deposited in stage 3. Devices were finished utilizing standard bath CdS, sputtered resistive ZnO, and sputtered ITO. Ni/Al grids and mechanical scribes were applied to form 1.16 $cm^2$ devices. All quoted device parameters are based on AM1.5, total-area measurements. No anti-reflective coating was applied to the devices in this study.

A summary of deposition conditions, CIGS properties, and device results for the samples in this study is given in Table 1. The samples form a three-level factorial experiment design with two factors (maximum Cu ratio, and moles in third stage) and several replicas. Final Ga ratio was controlled to 0.45 ± 0.05, while the final Cu ratio was controlled to 0.8 ± 0.7 and film thickness was kept between 2.1 and 3.4 μm. Some variations in thickness and final Cu ratio are necessary to achieve the desired combinations of maximum Cu ratio and third-stage atoms. The order of sample fabrication was randomized. In Table 1, maximum Cu ratio is abbreviated as "R2". Each row of Table 1 represents one CIGS substrate on which 12 devices were measured. The table lists both average and best-device parameters for each substrate. Evaluating deposition conditions by either choice of parameter is essentially equivalent, as the average and best-device parameter values are highly correlated.

Results of the factorial experiment were analyzed using Statistica® software.[11] The most important outputs from this analysis include, for each parameter listed in columns 2 through 9 of Table 1, an estimate of the magnitude of the two factors on the parameter, and level of statistical significance for these effects. Both linear and quadratic relationships between the factors and device parameters were explored. The level of statistical significance ("p-level") describes the probability for the particular relationship between the factors and device parameters, with lower p-levels indicating higher statistical significances. A p-level of 5% (0.05) is a typical threshold for concluding a relationship to be statistically significant at the 95% confidence level.

*Table 1: Sample and device characteristics.*

| Sample | Best device η (%) | Best device $V_{oc}$ (V) | Best device $J_{sc}$ (mA/$cm^2$) | Best device ff (%) | Avg η (%) | Avg $V_{oc}$ (V) | Avg $J_{sc}$ (mA/$cm^2$) | Avg ff (%) | Cu/ (In+Ga) | Ga/ (In+Ga) | thick-ness (μm) | R2 | Atoms ($10^{15}$/$cm^2$) |
|---|---|---|---|---|---|---|---|---|---|---|---|---|---|
| Low atoms - Low R2 | 8.7 | 0.533 | 24.7 | 0.66 | 7.9 | 0.543 | 23.3 | 0.62 | 0.73 | 0.39 | 2.1 | 0.85 | 354 |
| Low atoms - Ctr R2 | 8.5 | 0.619 | 21.2 | 0.64 | 7.9 | 0.613 | 20.4 | 0.63 | 0.76 | 0.49 | 2.2 | 1.05 | 365 |
| Low atoms - Ctr R2 | 10.3 | 0.591 | 26.9 | 0.65 | 8.1 | 0.580 | 22.9 | 0.61 | 0.8 | 0.44 | 2.2 | 1.04 | 367 |
| Low atoms - Hi R2 | 10.2 | 0.622 | 27.1 | 0.60 | 8.6 | 0.624 | 27.2 | 0.51 | 0.85 | 0.5 | 2.1 | 1.25 | 369 |
| Ctr atoms - Low R2 | 8.8 | 0.525 | 31.3 | 0.54 | 7.9 | 0.540 | 25.7 | 0.58 | 0.85 | 0.43 | 3 | 0.95 | 420 |
| Ctr atoms - Ctr R2 | 9.2 | 0.545 | 28.8 | 0.58 | 8.7 | 0.556 | 28.3 | 0.55 | 0.87 | 0.47 | 2.4 | 1.07 | 424 |
| Ctr atoms - Ctr R2 | 8.8 | 0.560 | 26.7 | 0.59 | 7.7 | 0.547 | 24.9 | 0.56 | 0.85 | 0.49 | 3.4 | 1.03 | 468 |
| Ctr atoms - Hi R2 | 10.3 | 0.598 | 27.3 | 0.63 | 9.5 | 0.603 | 25.3 | 0.62 | 0.87 | 0.48 | 2.4 | 1.11 | 466 |
| Hi atoms - Low R2 | 7.9 | 0.553 | 23.7 | 0.60 | 6.6 | 0.587 | 21.0 | 0.53 | 0.74 | 0.5 | 3.2 | 0.94 | 647 |
| Hi atoms - Ctr R2 | 9.7 | 0.566 | 26.1 | 0.66 | 8.6 | 0.527 | 27.1 | 0.60 | 0.83 | 0.45 | 2.1 | 1.05 | 591 |
| Hi atoms - Ctr R2 | 8.4 | 0.542 | 27.8 | 0.56 | 7.6 | 0.555 | 25.4 | 0.55 | 0.76 | 0.41 | 2.4 | 1.07 | 594 |
| Hi atoms - Hi R2 | 9.9 | 0.564 | 27.8 | 0.63 | 9.3 | 0.574 | 26.7 | 0.61 | 0.76 | 0.48 | 2.2 | 1.12 | 585 |

The statistically significant relationships are listed in Table 2. Effect magnitudes are defined as follows by the best fit surface for a parameter j to the data:

F(j, low k) ≡ the value of the fit to parameter j at the low value of factor k

Then for linear relationships,

Effect of factor k on parameter j ≡ F(j, high k) – F (j, low k)

and for quadratic relationships

Effect of factor k on parameter j ≡ F(j, center k) – ½ [F (j, low k)+ F (j, high k)]

Thus, a positive linear effect means the parameter increases with the factor, and a negative linear effect means the parameter increases as the factor decreases. Table 2 identifies a linear dependence of efficiency and $V_{oc}$ on maximum Cu ratio. A smaller dependence of $V_{oc}$ to decrease linearly with third-stage atoms is also identified. However, this dependence does not translate significantly to efficiency. The best fit surfaces for these significant dependencies are shown in Figure 1. Some curvature is apparent in the surfaces, however these quadratic terms are not statistically significant and therefore are not listed in Table 2.

*Table 2: List of statistically significant relationships from this study's data.*

| Parameter | Is a function of: | Form | Effect Magnitude | p-level |
|---|---|---|---|---|
| Average η | Maximum Cu ratio | Linear | 2.11 | 0.036 |
| Best device η | Maximum Cu ratio | Linear | 1.67 | 0.011 |
| Best device $V_{oc}$ | Maximum Cu ratio | Linear | 0.058 | 0.009 |
| Best device $V_{oc}$ | Stage 3 atoms | Linear | -0.035 | 0.042 |

Comparing this study with others in the literature requires consideration of both statistics and film growth kinetics. Shafarman et al[1] conclude that the Cu-rich growth period is beneficial only for devices deposited at reduced temperatures. However, two-stage, rather than three-stage growth was utilized. The simultaneous deposition of group I and III atoms during the two-stage process may provide more time for the necessary reactions and lessen the benefit of the Cu-rich growth period, since the benefit of the Cu-rich growth period has been surmised to come from a fluxing of the CIGS grains by excess liquid $Cu_2Se$.[9] Other conditions that affect film kinetics, such as the presence and amount of Na, are also expected to have an impact on the benefit of the Cu-rich growth period. It also should be noted that only six samples in the two-stage study (three at each of two temperatures) were used to draw conclusions. Nishiwaki et al[3] present one impressive efficiency (16.6%) formed by three-stage deposition without the Cu-rich growth period, but provide neither data from samples with Cu-rich growth nor data from replicas without Cu-rich growth.

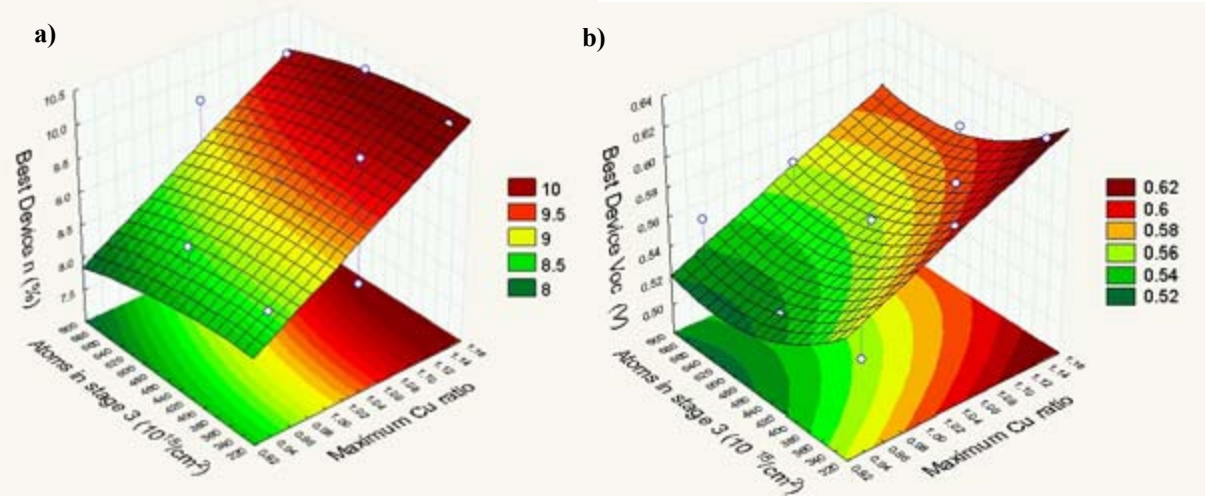


*Figure 1: Best-fit surfaces for a) efficiency and b) $V_{oc}$ as a function of maximum Cu ratio and atoms in stage 3.*

## 2.2 *Implications for Production*

As outlined above, for three-stage devices made in ITN's bell jar, a Cu-rich growth period was found to yield a statistically significant benefit on device performance. Given the sensitivity of bell jar devices to maximum Cu ratio, tests of the impact of maximum Cu ratio were also performed in the GSE production roll-coaters. A two-level screening test of maximum and final Cu ratio was executed. The $2 \times 2$ matrix was replicated one time for a total of eight test conditions. The planned levels for Cu-rich excursion were 1.0 and 1.1, as measured by in-situ XRF. The planned levels for final composition (Cu/(Ga+In)) were 0.81 and 0.91. The web was processed according to baseline manufacturing process conditions through production cell (i.e., large area devices, total area 78 $cm^2$) fabrication and measurement. Three thirty-cell sample panels were extracted from each condition. Deletion of outliers well outside the normal distribution was performed prior to analysis.

The mean efficiency of each condition are plotted on the interaction chart in Figure 2. For films processed without a Cu-rich excursion (in process Cu/(Ga+In) ~ 1.0), the final composition had a significant effect on final efficiency; a final Cu/(Ga+In) of 0.91 was superior to 0.81. All IV parameters ($V_{oc}$, $J_{sc}$, and fill factor) improved. For films that experienced a Cu-rich excursion (in process Cu/(Ga+In) ~ 1.1), the efficiency was much less dependent on the final Cu/(Ga+In). The latter process was more robust, although the mean efficiency under the best conditions may be slightly lower than the case where the film did not go Cu-rich.

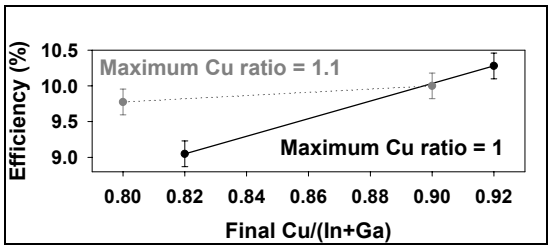


*Figure 2: Interaction chart summarizing device efficiency from roll-coaters as a function of maximum and final Cu ratio.*

As somewhat different conclusions were reached from the bell jar and roll-coater experiments, further examination of conditions in the roll-coater were performed. In these follow-up experiments, deposition temperature and film thickness (as varied either by source temperature or deposition time) were included as factors. Interpretation is more complex than for the earlier experiments, as – even for a constant maximum Cu ratio – thickness and resultant Ga profile impact performance. Substrate temperature is also a factor. These results are summarized in *Figure 3*, showing efficiency as a function of the newly-introduced factors, for constant maximum Cu ratio. The legend lists the process conditions for each symbol. Analysis of the designed experiment and resulting error bars were generated using Statistica®[11] software.

Thus, despite the demonstrated benefit of a Cu-rich growth period for bell jar devices, designed experiments performed in production roll-coaters determined that the effect of maximum Cu ratio is convoluted with film thickness, temperature, and time. Future efforts are to be directed toward fully optimizing conditions and assigning the inter-dependencies to physical mechanisms such as the Ga profile.

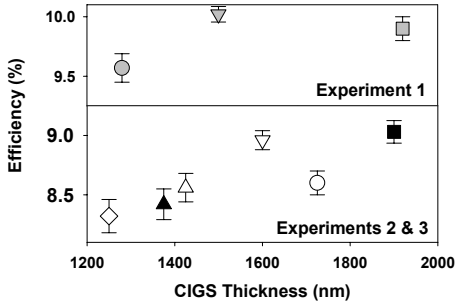


| Data Point | Web T | Source T | Web Speed | Max. Cu ratio |
|---|---|---|---|---|
| ○ | High | High | High | Constant |
| ▽ | High | High | Medium | Constant |
| □ | High | High | Low | Constant |
| ▲ | High | Low | Medium | Constant |
| ■ | High | High | Medium | Constant |
| ○ | Low | High | Medium | Constant |
| ▽ | High | High | Medium | Constant |
| ◇ | High | High | High | Constant |
| △ | Low | High | High | Constant |

*Figure 3: Results from experimental design varying deposition temperature and CIGS thickness (by source temperature or web thickness) in roll-coaters, at constant Cu ratio.*

# 3 Film Growth

## *3.1 Bell Jar Studies*

Process sensitivities related to film growth kinetics (e.g., as shown in the previous chapter for the extent of Cu-rich excursion) might be expected to exhibit significant inter-dependencies. Hence, traditional stationary bell-jar depositions cannot be compared to dynamic RTR production conditions unless the latter can be reproduced in a stationary system. As the associated costs and inherent sluggish response of large production systems to parameter changes inhibits fast and inexpensive exploration of the vast parameter space of multi-source co-evaporation of CIGS, a small scale, low-cost R&D approach is highly desirable. Once the main interactions and most significant process variables have been identified, process optimization can then proceed at the production scale in a more economical fashion.

Depositions were conducted in order to develop a procedure to mimic the GSE roll coater time-temperature (t-T) and flux profiles in the ITN bell jar. Initial depositions employing very fast deposition rates onto steel substrates, which simulate the high throughput in the production roll-coaters, indicated a possible sensitivity of device results to temperature ramp rate, which can be much faster for thin steel substrates than the typically-used higher thermal mass glass. Subsequently 4 factor, 2 level (one complete replica) experiments were performed to mimic the GSE process in the ITN bell jar and to determine the effect of selective process variables – stage 1-2 temperature ramp time, ramp end time of 2$^{nd}$ stage, stage 2 and 3 temperature (treated as 1 variable), and deposition rate – on device performance.

Initial attempts to control the deposition on GSE provided substrate were unsuccessful, yielding wide fluctuations in composition. The main difficulty seemed to originate from an abnormal IR signal precluding endpoint detection after the 2$^{nd}$ stage. The samples in this set displayed emissivity increases that began at very low Cu ratio at the beginning of stage 2. Apparently some high-emissivity compound, other than the usual excess $Cu_2Se$, formed in the film. Figure 4 compares a normal IR signal for stage 2 and 3 to the abnormal signal returned in the initial deposition series.

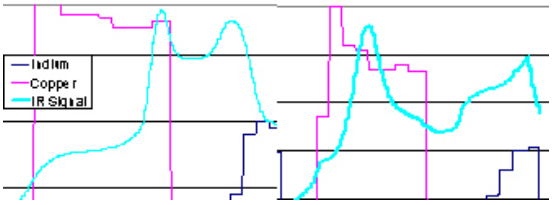


*Figure 4: Desired (left) and undesired (right) IR profile for a GSE mimic deposition at ITN.*

This unexpected complication necessitated that we identify possible causes. We proceeded by compiling a trouble-shooting list and tackling each subsequent item one by one. While some minor corrections to sensors resulted, none of the other items yielded out-of spec parameters nor did the IR signal improve. Subsequently, the t-T-flux profile was broken down into smaller segments with unchanged components based on the ITN baseline process. This approach restored the normal IR signal and yielded devices on SS in the 8.4 to 8.6% range with up to 75% of the t-T-flux profile matched to the GSE condition. Subsequent attempts at increased rates and decreased times to match 87.5% of the GSE profile once again yielded the abnormal IR signal, while repeats at the 75% match level resulted in normal sensor signals.

At this point it is not clear why IR signal endpoint detection fails to work if process times are reduced and fluxes increased to simulate GSE's production process in a stationary, fixed source-substrate geometry bell-jar environment. In the interest of cost and time, all future process tolerance work was to be conducted on the actual production equipment.

## *3.2 Production Ga/(Ga+In) Profile*

Although considerable progress had been made in achieving reproducible production yields and mean cell efficiency in the roll coaters, further improvements were desired. All coating processes were under investigation to

understand their effect on reproducibility, but the CIGS process received the most attention. The CIGS process has historically been the largest contributor to production output noise. Process drift during the course of a single CIGS run and XRF calibration error lead to measurable inter- and intra-lot composition variation. Tests were conducted to understand the tolerance of the CIGS process for composition variations and to identify hardware and process setpoint modifications to improve the output tolerance for these variations.

The focus of the tests conducted was the Ga/(Ga+In) profile through the film thickness. In three-stage depositions conducted in bell jars, virtually all Ga/(Ga+In) profiles possible can be achieved through independent control of the Ga and In fluxes to the fixed substrate. In the production roll coaters, however, limitations in achievable profiles are imposed by the nature of the continuous roll coating process. Discrete effusion sources for each element at fixed locations are specifically responsible.

Modifications were made to the standard effusion sources for the tests that provide better mixing of the elemental fluxes. The location of these modified effusion sources and their respective elemental fluxes were the test variables. Six tests were conducted on webs each 800 feet and containing 20 test conditions. The standard test condition was forty feet in length. Tests were designed using standard matrices for 2 variables, 3 levels each ($3 \times 3$) with single or double replicates. Within the entire test series approximately the same test parameters (besides location) were applied to each lot. Besides the CIGS test conditions, webs were processed under standard conditions in all remaining thin film coating steps. Three panels with 12 cells each (68.8 $cm^2$) were selected from each test condition for measurement.

A summary of the six test lots is shown in Table 3. The mean maximum efficiency and best uniformity between test conditions (tolerance) was obtained for configurations B and E. $V_{oc}$ and $I_{sc}$ had excellent model fits within each lot. Fill factor was fit poorly, indicating that fill factor was not strongly affected by the test parameters. A comparison between $I_{sc}$ and $V_{oc}$ for each test lot confirmed the superiority of configurations B and repeat of C for the $I_{sc} \times V_{oc}$ product (Figure 5). While configuration B appears to offer the best compromise, all of the non-standard four configurations explored are capable of achieving maximum efficiencies in the 9.6 to 10.2% range. Tests to further down-select between the more process tolerant configurations B and E as opposed to the condition C, resulting in the highest efficiencies, are planed for the future.

*Table 3: Cell performance summary for test lots.*

| Lot | Config. | Maximum $\eta$ (%) | $V_{oc}$ at Max. $\eta$ (mV) | $I_{sc}$ at Max. $\eta$ (mA) | FF at Max. $\eta$ (%) | Average $\eta$ (all Tests) |
|---|---|---|---|---|---|---|
| 1786SA | A | 9.15 | 531 | 2090 | 56.7 | 8.48 |
| 1793SA | B | 9.78 | 559 | 2167 | 55.5 | 9.53 |
| 1807SA | C | 8.73 | 540 | 2058 | 54.0 | 7.65 |
| 1826SA | D | 9.61 | 574 | 1997 | 57.7 | 9.09 |
| 1839SA | E | 9.85 | 556 | 2177 | 56.0 | 9.49 |
| 1841SA | C | 10.20 | 544 | 2223 | 58.0 | 9.57 |

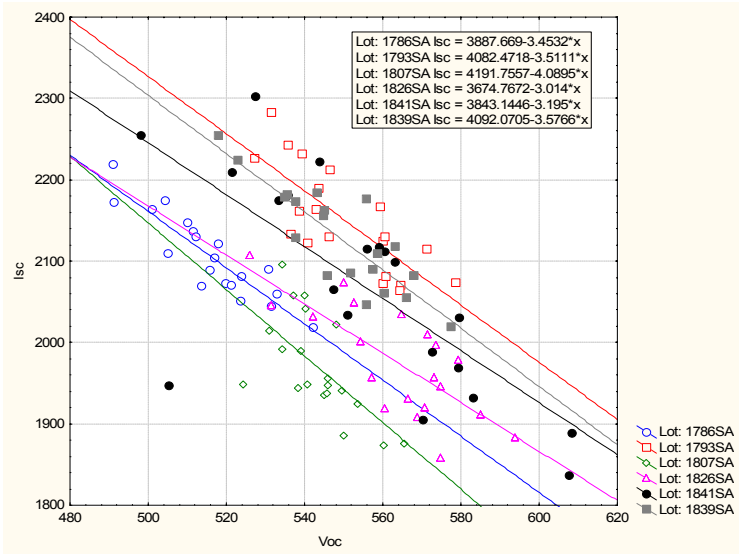


*Figure 5: $I_{sc}$/$V_{oc}$ characteristics of In/Ga flux test lots.*

## *3.3 Production $T_{sub}$ and Na Precursor Sensitivity*

Improvements in efficiency and yield due to enhanced adhesion of the absorber to the back contact were targeted via a 4 factor, 2 level experiment including center points. Evaluation of the parameter space was conducted in two independent depositions spread over two CIGS roll coaters. The experimental portion of each deposition was 800 ft. containing 18 conditions. Following device completion 5 panels yielding 12 cells each were removed from each of the 18 conditions. Statistical analysis under removal of outliers showed the strongest impact to be the substrate temperature during Na precursor deposition. As illustrated in Figures 6 and 7 a significant improvement in CIGS adhesion as well as efficiency as a function of Na precursor deposition conditions is evident. Furthermore, optimization of the Na precursor deposition step resulted in a more robust process.

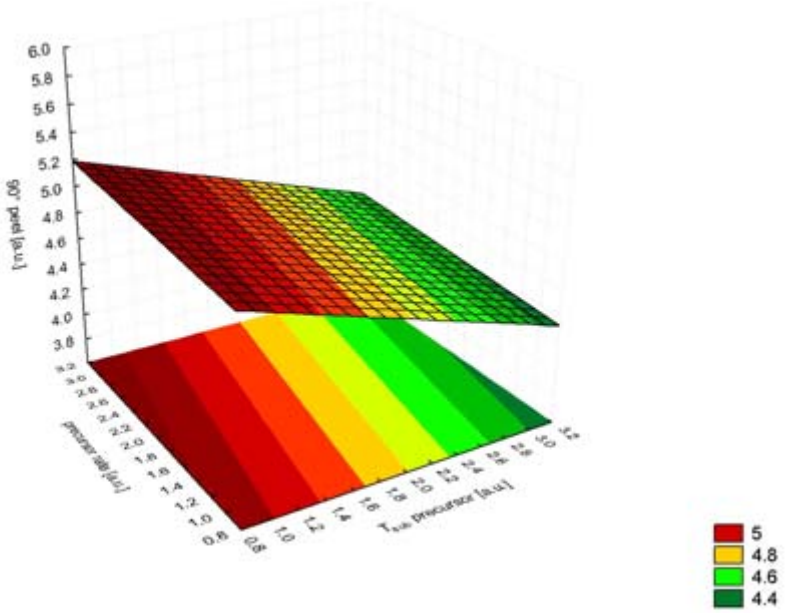


*Figure 6: Fitted surface of CIGS to back contact adhesion as a function of $T_{sub}$ during precursor deposition and rate.*

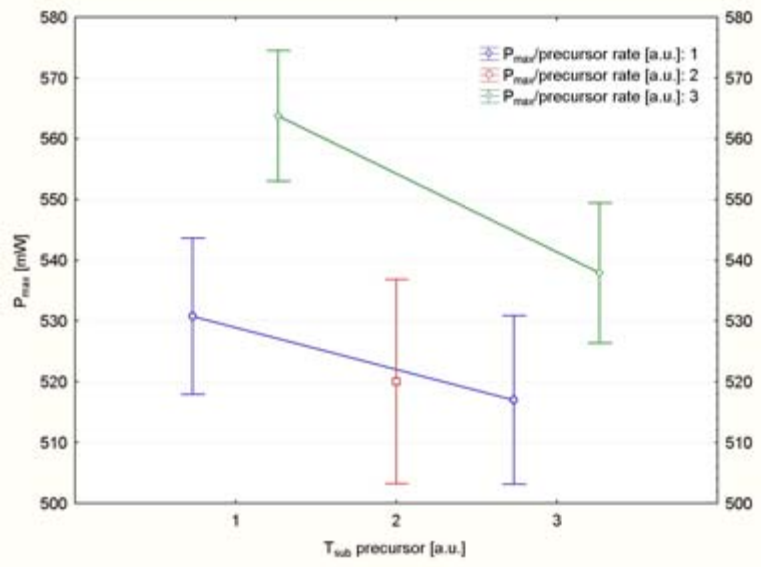


*Figure 7: $P_{max}$ as a function of $T_{sub}$ during Na precursor deposition and rate.*

### *3.4 Production Se Delivery Rate Sensitivity*

In addition to the already explored process sensitivities, statistical analysis of all thin film coating (TFC) processes traced inter-lot variations to the specific CIGS coaters. In section 3.2 efforts investigating the tolerance of the CIGS process to composition variation of the group III elements throughout the absorber layer have been discussed. With two of the four CIGS coaters configured to the best set resulting from this test series, screening experiments were conducted to identify the key – not directly composition driven – parameters responsible for the coater-based deviation. Experiments confirm that the process is well centered in the optimal parameter space for the variables tested. As an example, Figure 8 demonstrates the response to a change in Se delivery rate with the medium level corresponding to the current baseline process. Due to the nature of screening experiments, the width of the plateau cannot be obtained, while the design chosen still allowed for confirmation of curvature and computation of effect estimates.

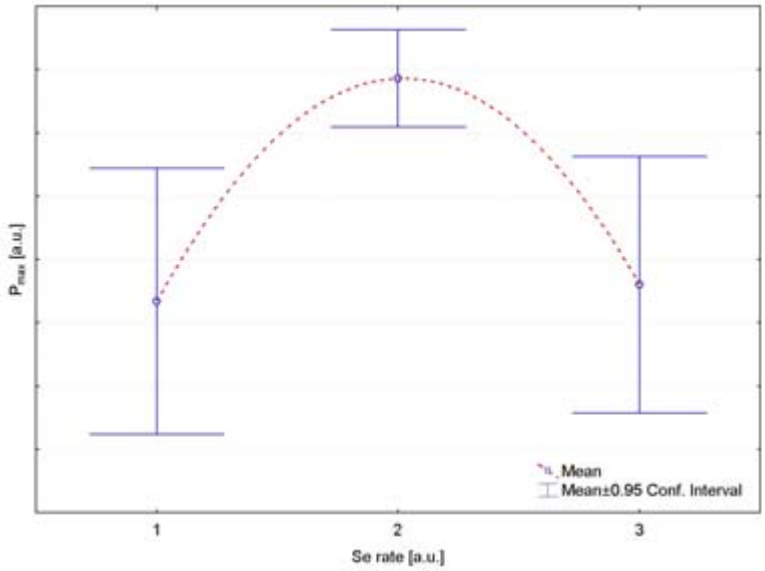


*Figure 8: Average production cell power as a function of Se rate delivery.*

# 4 Post-Deposition Treatments

Post-deposition treatments of production CIGS have been examined for a boost to efficiency and process robustness in two forms: surface sulfurization via thioacetamide and, post-deposition Na treatments following recent work by Rudmann et al.[12]

Over the past several years, two CIGS groups have reported relative device efficiency increases of as much as 20% due to an additional chemical treatment involving solutions containing thioacetamide.[13,14] The efficiency improvement has been attributed to the formation of a thin sulfide layer and/or surface passivation by sulfur atoms. Thioacetamide treatments were evaluated on GSE production material by designed experiment. Treatment time, temperature, and concentrations were varied. Although optimum conditions were found to be consistent with those in the literature, no statistically significant performance benefit was realized compared to untreated samples. Figure 9 shows a box and whisker plot of the efficiency for thioacetamide treated samples (0) and untreated devices (1). Although not statistically significant, the mean efficiency of the untreated specimens is slightly higher than for the treated samples. Furthermore, a narrower distribution for the untreated samples is evident from the standard deviation (SD), indicating poor reproducibility of the thioacetamide process. Due to the larger number of treated devices the standard error (SE) is narrower as compared to the untreated absorbers. Representative IV plots further illustrate that no significant difference can be observed between the two device groups (Figure 10: ). It was concluded that the benefit of the thioacetamide treatment is dependent either on some property of the CIGS surface not present in the GSE material, or on a procedural detail not reproduced in our experiments.

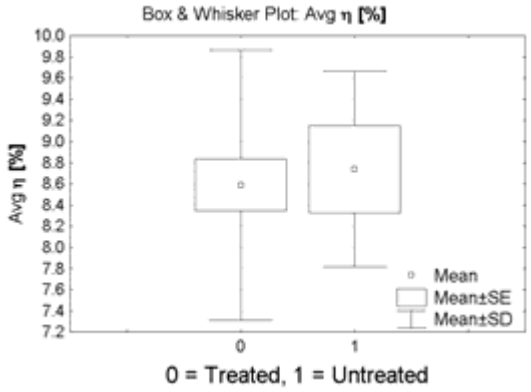


*Figure 9: Box and whisker plot of efficiency for thioacetamide treated samples and control devices.*

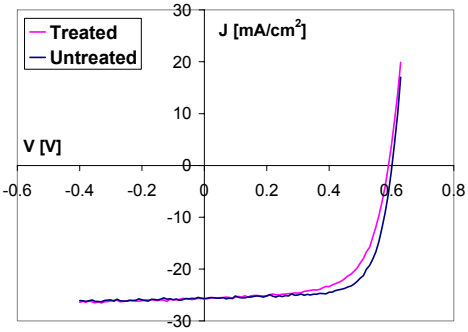


*Figure 10: Representative current-voltage trace for a treated and an untreated device.*

Passivation of CIGS on flexible substrates by treatment with NaF has also been reported.[12] Post absorber formation Na treatment was applied to production-line CIGS at GSE for absorbers prepared on steel under various deposition conditions. The two types of material were subsequently sent to ITN for post-absorber treatment. Herein, a portion of each coupon set was treated with a Na compound and finished into devices, while another portion was finished into devices without post-absorber Na treatment. Treatment time and temperature were

examined as variables in the designed experiment. Optimum conditions were found to be consistent with those in the literature. Results for coupons 15 and 55, treated under the conditions reported by Rudmann, are shown by the blue bars in Figure 11. For both coupons sets – particularly for the lower efficiency material – the post-deposition Na passivation increases efficiency. GSE is investigating concepts to better implement and test passivation via Na on the production scale level.

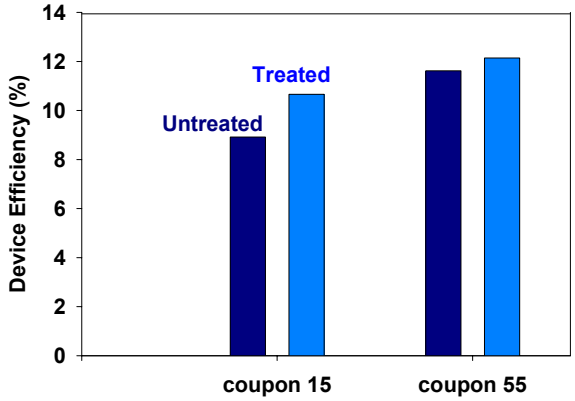


*Figure 11: CIGS device efficiencies with and without exposure to post-deposition treatment.*

# 5 Feedstock Purity

High-efficiency CIGS devices made in R&D laboratories are based on absorber depositions employing the highest purity source materials available. The option to utilize lower purity feedstock would benefit industry in terms of lower materials cost and better availability. However, as the impact of increasing impurity content in the source materials on device performance has not been explored, experiments to this effect are necessary to exclude potential shortfalls in device quality – e.g., due to the introduction of electronic defects. The ultimate goal was to find the most economic compromise between materials cost (purity) and resulting device performance.

Prior to the actual experimentation, a survey was conducted to obtain information on (a) the source purity of Cu, In, Ga, and Se employed at NREL, ITN, and GSE; (b) the commercially available lower and upper end purities for these 4 elements; and (c) the respective unit costs per element for these categories. Based on up to 4 vendors per element, Table 4 summarizes average expenses or savings when moving to higher or lower feedstock purities by one ninth. For example, almost no savings result in switching to lower purity Se, compared to significant cost impacts for higher or lower purity Cu and In. Thus, investigating the effect of changing Cu and In purity was assigned a higher priority than changes in Se purity.

*Table 4: Expenses or savings expected from increasing or decreasing source purity by one ninth.*

| Element | Increase by one 9: Savings [$/g] | Decrease by one 9: Savings [$/g] |
|---|---|---|
| Cu | -1.05 | 1.35 |
| In | -1.04 | 0.60 |
| Ga | -0.53 | Not available |
| Se | Not available | 0.03 |

Subsequent to the above, a single-factor (metals purity), three-level experiment was designed; the characteristics of each level are summarized in Table 5. A few aspects of Table 5 merit further explanation.

- *Se was excluded from the experiment,* as ITN, GSE, and NREL utilize the same purity feedstock and higher purity Se is not readily available, while lower purity Se offers negligible cost savings.
- *The "low" level of Ga purity is the same as the "medium" level,* as lower purity Ga was not available from any of the vendors surveyed.
- *The "high" levels of purity for Cu and Ga exceed the "medium" level by 2, rather than 1, ninth.* The goal of the study was to screen for maximum effects, hence the widest possible purity range was explored starting from the most pure material down.

*Table 5: Metals purity levels.*

| Level | Cu purity (#9's) | In purity (#9's) | Ga purity (#9's) | Se purity (#9's) |
|---|---|---|---|---|
| Low | 3 | 4 | 4 | N/A |
| Medium | 4 | 5 | 4 | N/A |
| High | 6 | 6 | 6 | N/A |

In order to exclude substrate or process based convoluting factors, depositions were on Mo-coated glass substrates with three-stage CIGS deposited over approximately 20 minutes, using film emissivity endpoint detection for stages 2 and 3. The atomic Ga/(Ga+In) ratio was kept constant ± 2.5%. Each condition included one replica and the resulting device parameters are summarized in Table 6. Statistical analysis of the complete device data set, as well as QE analysis, revealed the majority of the efficiency loss in the lower purity samples to be due to a shortfall in $J_{sc}$ (mostly in the red portion of the spectrum) while $V_{oc}$ and FF seem unaffected by source purity (Figure 12). Significant differences were only obtained for the low purity device set, while no statistically significant gain was evident when switching from medium quality metals to the highest purity level.

*Table 6: Best device parameters.*

| purity | Best device η [%] | Best device $V_{oc}$ [mV] | Best device $J_{sc}$ [mA/cm$^2$] | Best device FF [%] |
|---|---|---|---|---|
| Low | 7.12 | 513 | 22.76 | 61 |
| Low | 8.83 | 570 | 23.35 | 66 |
| Medium | 11.18 | 612 | 26.31 | 70 |
| Medium | 10.78 | 582 | 28.62 | 67 |
| High | 10.82 | 534 | 32.83 | 64 |
| High | 10.00 | 572 | 28.71 | 63 |

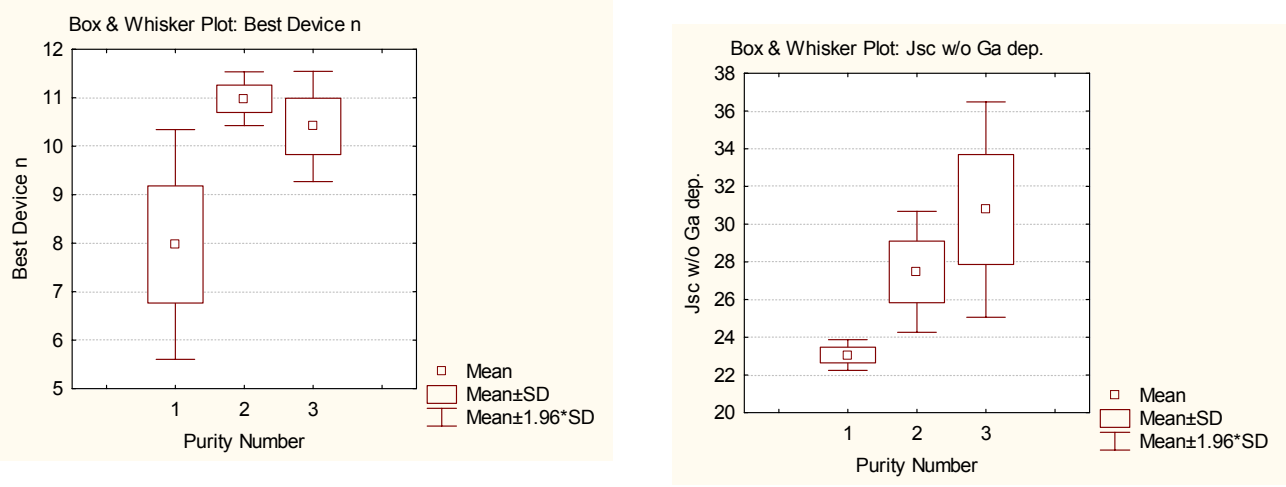


*Figure 12: Box and Whisker plots of efficiency (left) and $J_{sc}$ (right) versus source purity.*

# 6 Further Production Sensitivities

Building on past efforts to realize further improvements in production yield and increased device efficiency, all thin film coating (TFC) steps were further scrutinized. Statistical evaluation of production data as a function of process and TFC system combination revealed minor variations despite nominally identical hardware and setpoint values per TFC process.

While the CIGS process has historically been found to be the most significant contributor to production output noise, the above analysis warranted a closer look at the first process step, the back contact deposition. Via the design of experiment (DOE) approach sensitivities have been confirmed and traced to physical properties of the

back contact. Further work lead to a practical solution to address the process variability, subsequently narrowing the device efficiency distribution and increasing yield (Figure 13) due to improved intra-run uniformity.

Further back contact related work was directed at improving CIGS to back contact adhesion beyond the optimization obtained via modifications to the CIGS depositon process – in particular the Na precursor deposition step as discussed under section 3.3. In addition, device improvements due to enhanced diffusion barrier properties of alternate back contact schemes were targeted. Various back-contact film structures were evaluated in combination with process parameter changes for the more promissing material layer sequences and compared to the optimized standard back contact.

SIMS depth profilies were generated on the standard back contact as well as an altrernate layer sequence at two different thicknesses. Figure 14 illustrates that Fe diffusion from the SS into the CIGS is effectively prevented by all three back contacts. On the other hand, as the bright green line (Cr 400) in Figure 14 demonstrates, Cr diffuses into the CIGS for the standard back contact structure. Employing the alternate back contact under investigatrion Cr diffusion into the CIGS can be effectively blocked. In addition, marginal improvements in CIGS to back contact adhesion over the standard layer could be achieved with this new structure. Unfortunately, the resulting devices showed a significantly reduced performance.

In subsequent tests the Cr diffusion supressing layer position in the stack was altered. Two new layer sequences were investigated and the resulting device performance compared to the standard back contact. Analysis of the impact of each back contact film stack on cell efficiency is summarized in Figure 15 – #1 denotes the standard GSE back contact. The only statistically significant difference was a slight decrease for the alternate constructions. The difference, however, is small (only ≈ about 0.6%) and may be partially attributable to any number of unrelated factors encountered during cell fabrication. Alternatively, the thickness of the diffusion barrier layer may not be optimized, nor may the actual layer sequence.

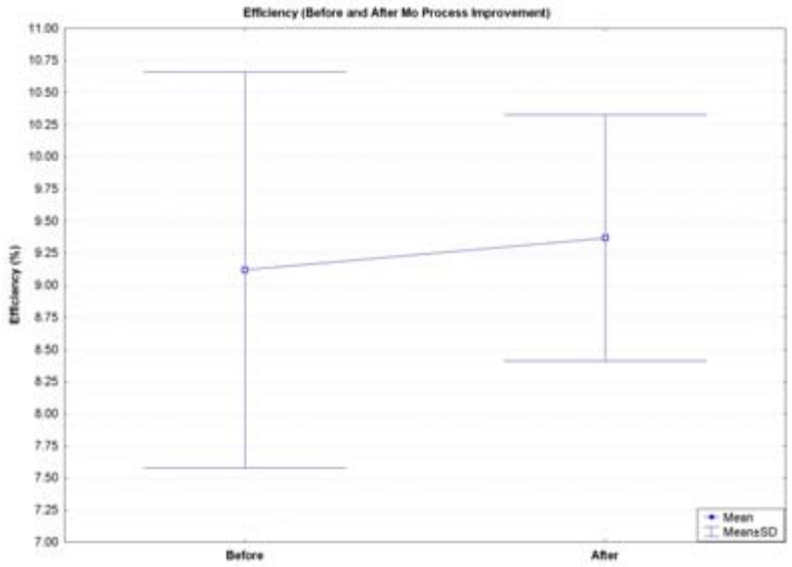


*Figure 13: Distribution and average efficiency before and after Mo process optimization.*

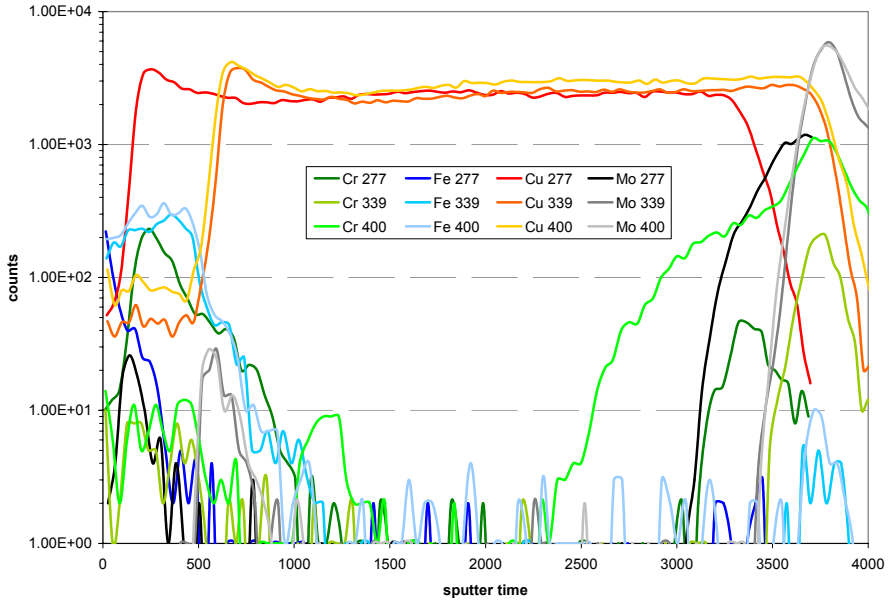


*Figure 14: SIMS depth profile through standard back contact (400), and an alternate back contact sequence of two different thicknesses (277 and 339).*

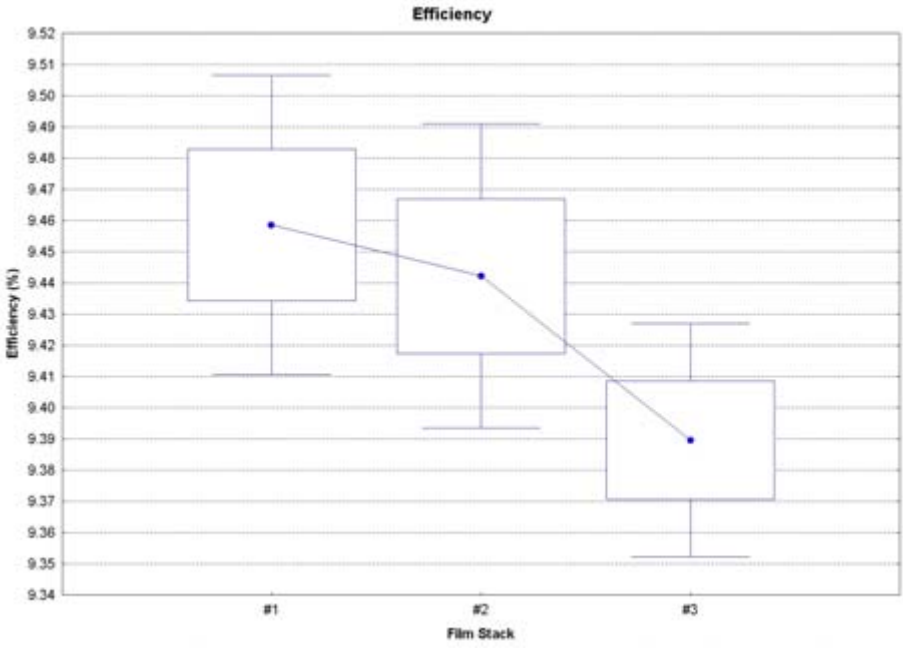


*Figure 15: CIGS device efficiency as function of back contact type – #1 denotes the standard GSE back contact.*

# 7 Technical Summary

Work during Phase III progressed in several key areas, primarily focused on the production scale processes:

- process sensitivities to the degree of Cu-rich excursion,
- Ga/(In+Ga) distribution throughout the absorber,
- Na precursor deposition step,

- Se delivery,
- Back contact optimization,
- Feedstock purity impacts, and
- Surface passivation.

The following conclusions were drawn related to production:

- A maximum Cu ratio of 1.1 is more robust than a maximum Cu ratio of 1.0.
- Various Ga/(In+Ga) distributions throughout the absorber yield maximum efficiencies, but a robust process can be achieved for a narrow group III distribution only.
- Na precursor deposition conditions are instrumental to absorber adhesion as well as device performance.
- Insufficient as well as excessive Se delivery negatively impacts device performance.
- Cr diffusion into the absorber can effectively be blocked while simultaneously enhancing CIGS adhesion.
- No gains in efficiency can be expected from increased feedstock purity while reduced feedstock purity would result in significant losses.
- For the present GSE absorber surface sulfurization is not a viable option to replace CdS.
- Stationary bell jar experiments cannot adequately simulate the dynamics in RTR film growth.

# 8 Team Activities

GSE participated in National CIS R&D Team activities. Recent contributions have included participation in and presentations at team meetings, submission of samples for comparative absorber studies, and review and discussion of related data.

# 9 Phase III Publications, Presentations, and Reports

The following publications, presentations, and reports were generated related to this contract during Phase III. They are listed in chronological order:

1. Phase III, First Quarterly Report, August 19, (2004).
2. M.E. Beck, I.L. Repins, J.S. Britt, "Sensitivities in Roll-to-Roll Processing of CIGS-Based Photovoltaics on Flexible Metal Foils", DOE Solar Program Review Meeting, October 25-28, (2004).
3. W.K. Batchelor, I.L. Repins, J. Schaefer, and M.E. Beck, "Impact of substrate roughness on $CuIn_xGa_{1-x}Se_2$ device properties", Solar Energy Mater. Sol. Cells, 83 (2004) 67-80.
4. Phase III, Second Quarterly Report, November, 15, (2004).
5. M.E. Beck, S. Wiedeman, R. Huntington, J. VanAlsburg, E. Kanto, R. Butcher, and J.S. Britt, "Advancements in Flexible CIGS Module Manufacturing", 31st IEEE PVSEC, (2005).
6. I.L. Repins, D.C. Fisher, M.E. Beck, and J.S. Britt, "Effect of Maximum Cu Ratio During Three-Stage CIGS Growth Documented by Design of Experiment", 31st IEEE PVSEC, (2005).
7. D.C. Fisher, I.L. Repins, J. Schaefer, M.E. Beck, W.K. Batchelor, M. Young, and S. Asher, "The Effect of Mo Morphology on the Performance of $Cu(In,Ga)Se_2$ Thin Films", 31st IEEE PVSEC, (2005).
8. W.K. Batchelor, M.E. Beck, and I.L. Repins, "Variations of Thioacetamide Treatments on CIGS Solar Cells on Stainless Steel Substrates – Correlations to Device Performance", 31st IEEE PVSEC, (2005).
9. Phase III, Third Quarterly Report, February 28, (2005).

10. I.L. Repins, D. Fisher, W.K. Batchelor, L. Woods, and M.E. Beck, "A Non-Contact Low-Cost Sensor for Improved Repeatability in Co-Evaporated CIGS", Prog. Photovolt. Res. Appl., 13 (2005) 311-323.

11. Phase III, Fourth Quarterly Report, May 23, (2005).

# 10 References

[1] W.N. Shafarman, R.W. Birkmire, S. Marsillac, M. Marudachalam, N. Orbey, T.W.F Russell, "Effect of Reduced Deposition Temperature, Time, and Thickness, on Cu(In,Ga)$Se_2$ Films and Devices", *Conference Record of the 26th IEEE Photovoltaic Specialists Conference*, pp.331-334, (1997).

[2] W.N. Shafarman, J. Zhu, "Effect of Substrate Temperature and Deposition Profile on Evaporated Cu(In,Ga)$Se_2$ films and devices", *Thin Solid Films* **361-362**, pp. 473-477, (2000).

[3] S. Nishiwaki, T. Satoh, S. Hayashi, Y. Hashimoto, T. Negami, T. Wada, "Preparation of Cu(In,Ga)$Se_2$ thin films from In-Ga-Se Precursors for high-efficiency solar cells", *Journal of Materials Research* **14** (12), pp. 4514-4520, (1999).

[4] J.R. Tuttle, T.A. Berens, J. Keane, K.R. Ramanathan, J. Granata, R.N. Bhattacharya, H. Wiesner, M.A. Contreras, R. Noufi, "Investigations into Alternate Substrate, Absorber, and Buffer Layer Processing for Cu(In,Ge)$Se_2$ – Based Solar Cells", *Conference Record of the 25th IEEE Photovoltaic Specialists Conference*, pp.797-800, (1996).

[5] J.E. Granata, "The Impact of Deliberate Sodium Incorporation on $CuInSe_2$-Based Solar Cells", Unpublished Ph.D. Thesis, Colorado State University, (1999).

[6] M. Bodegard, J. Kessler, O. Lundberg, J. Scholdstrom, L Stolt, "Growth of Co-Evaporated Cu(In,Ga)$Se_2$ – The Influence of Rate Profiles on Film Morphology," *Materials Research Society Symposium Proceedings*, **668**, (2001), pp. H2.2.1-H2.2.12.

[7] A.M. Gabor, J.R. Tuttle, D.S. Albin, M.A. Contreras, R. Noufi, A.M. Herman, "High-efficiency $CuIn_xGa_{1-x}Se_2$ solar cells made from $(In_x,Ga_{1-x})_2Se_3$ precursor films", *Applied Physics Letters*, **65**(2), pp. 198-200, (1994).

[8] D. S. Albin, G.D. Mooney, A. Duda, J. Tuttle, R. Matson, R. Noufi, *Solar Cells* **30**, 47, (1991).

[9] B. M. Keyes, P. Dippo, W. Metzger, J. AbuShama, R. Noufi, "Cu(In,Ga)$Se_2$ Thin Film Evolution During Growth – A Photoluminescence Study", *Conference Record of the Twenty-Ninth IEEE Photovoltaics Specialists Conference*, (2002).

[10] See, for example, G.E.P. Box, W.G. Hunter, J.S. Hunter, *Statistics for Experimenters*, John Wiley & Sons, (1978), pp. 289 ff.

[11] http://www.statsoft.com/textbook/stathome.html

[12] D. Rudmann, D. Bremaud, H. Zogg, A.N. Tiwari, "Na Incorporation for Low Temperature Cu(In,Ga)$Se_2$ Growth," *Proceedings of the 19th European PVSEC*, (2004).

[13] T. Nakada, K. Matsumoto and M. Okumura. "Improved Efficiency of Cu(In,Ga)$Se_2$ Thin Film Solar Cells by Surface Sulfurization Using Wet Process", Proc. of the 28th IEEE PVSC, (2002), p. 527.

[14] T. Wada, Y. Hashimoto, S. Nishiwaki, T. Satoh, S. Hayashi, T. Negami and H. Miyake. "High-efficiency CIGS Solar Cells with Modified CIGS Surface", Solar Energy Materials and Solar Cells, **67** (2001) p. 305.

# REPORT DOCUMENTATION PAGE

*Form Approved*
*OMB No. 0704-0188*



**PLEASE DO NOT RETURN YOUR FORM TO THE ABOVE ORGANIZATION.**

| 1. REPORT DATE *(DD-MM-YYYY)* | 2. REPORT TYPE | 3. DATES COVERED *(From - To)* |
|---|---|---|
| January 2006 | Subcontract Report | May 2003 – September 2005 |

**4. TITLE AND SUBTITLE**
Tolerance of Three-Stage CIGS Deposition to Variations Imposed by Roll-to-Roll Processing: Final Technical Report, May 2003 – September 2005

**5a. CONTRACT NUMBER**
DE-AC36-99-GO10337

**5b. GRANT NUMBER**

**5c. PROGRAM ELEMENT NUMBER**

**6. AUTHOR(S)**
M.E. Beck and J.S. Britt

**5d. PROJECT NUMBER**
NREL/SR-520-39119

**5e. TASK NUMBER**
PVB65105

**5f. WORK UNIT NUMBER**

**7. PERFORMING ORGANIZATION NAME(S) AND ADDRESS(ES)**
Global Solar Energy, Inc.
5575 South Houghton Road
Tucson, Arizona 85747

**8. PERFORMING ORGANIZATION REPORT NUMBER**
ZDJ-2-30630-14

**9. SPONSORING/MONITORING AGENCY NAME(S) AND ADDRESS(ES)**
National Renewable Energy Laboratory
1617 Cole Blvd.
Golden, CO 80401-3393

**10. SPONSOR/MONITOR'S ACRONYM(S)**
NREL

**11. SPONSORING/MONITORING AGENCY REPORT NUMBER**
NREL/SR-520-39119

**12. DISTRIBUTION AVAILABILITY STATEMENT**
National Technical Information Service
U.S. Department of Commerce
5285 Port Royal Road
Springfield, VA 22161

**13. SUPPLEMENTARY NOTES**
NREL Technical Monitor: H.S. Ullal

**14. ABSTRACT** *(Maximum **200 Words**)*

Three-stage co-evaporation of CIGS imposes stringent limits on the parameter space if high-efficient devices are to result. Substrate temperatures during the 1st stage (as well as during the 2nd and 3rd stage), Se partial pressure, and amount of Na supplied are critical for good nucleation, proper In-Ga-selenide precursor phase, and diffusion of Cu into the precursor, as well as diffusion of Ga through the film. In addition, the degree of Cu-rich excursion impacts maximum performance and process tolerance. Enveloping the above is the basic time-temperature profile inextricably linked to the metals delivery rates. Although high-efficiency, three-stage deposited CIGS devices on the R&D scale are grown at about 20-45 minutes to thicknesses of 2 to 2.5 μm, the latter is not a viable approach for an economic manufacturing process. At Global Solar Energy, Inc., CIGS films are typically grown in about 6 minutes to thicknesses of less than 2 μm. At the same time, the emissivity and thermal conductivity of stainless steel is vastly different from that of glass, and the reduced growth time poses restrictions on the substrate temperature ramp rates and diffusion of species (reaction kinetics). Material compatibility in the highly corrosive Se environment places limitations on the substrate heaters; i.e., substrate temperatures. Finally, one key advantage of a RTR deposition approach (compact equipment) restricts post CIGS Se exposure and cool-down rates to be vastly different than those practiced in the laboratory.

**15. SUBJECT TERMS**
PV; three-stage co-evaporation; roll-to-roll (RTR) processing; CIGS; high-efficient devices; module;

| 16. SECURITY CLASSIFICATION OF: | | | 17. LIMITATION OF ABSTRACT | 18. NUMBER OF PAGES | 19a. NAME OF RESPONSIBLE PERSON |
|---|---|---|---|---|---|
| a. REPORT | b. ABSTRACT | c. THIS PAGE | | | |
| Unclassified | Unclassified | Unclassified | UL | | 19b. TELEPONE NUMBER (*Include area code*) |